ELSEVIER

A microdrive track following controller design using robust and perfect tracking control with nonlinear compensation

Guoyang Cheng, Kemao Peng, Ben M. Chen *, Tong H. Lee

Department of Electrical and Computer Engineering, The National University of Singapore, Singapore 117576, Singapore

Abstract

Pivot bearing friction and flex cable nonlinearity are the two major torque nonlinearities which lead to performance degradation in hard disk drive (HDD) tracking tasks. Based on a comprehensive model of typical voice-coil-motor (VCM) actuator, which explicitly captures the characteristics of pivot bearing friction and flex cable nonlinearity, this paper presents the design of a parameterized controller for a microdrive using the robust and perfect tracking (RPT) technique combined with nonlinear torque compensation and integral enhancement. Simulation and experimental results show that the controller is capable of achieving fast settling and eliminating static bias.
© 2005 Elsevier Ltd. All rights reserved.

Keywords: Hard disk drives; Servo systems; Robust and perfect tracking; Control applications

---

* Corresponding author. Tel.: +65 68742289; fax: +65 67791103.
E-mail addresses: engp1496@nus.edu.sg (G. Cheng), elepkm@nus.edu.sg (K. Peng), bmchen@nus.edu.sg (B.M. Chen), eleleeth@nus.edu.sg (T.H. Lee).

1. Introduction

Current trend of the hard disk drive (HDD) industry is towards small and micro disk drives, for increasing applications in consumer electronics, such as digital cameras and music players. While HDDs are getting smaller in size (or the so-called form factor), their capacities are constantly on the rise, which means higher track density on disks. Track density is measured by TPI (track per inch), and its reciprocal is the so-called track pitch. To ensure reliable data reading and writing, it is required that during track following stage, the deviation of read/write (R/W) head from target track center, or the so-called track mis-registration (TMR), should not exceed 5% of track pitch, which is about 0.025 μm for a 50 kTPI HDD. This is one of the objectives in the HDD servo system design. To this end, various control techniques have been proposed, ranging from conventional PID control, lead–lag compensation, notch filters, and disturbance observer (see, for example, [10]), to more advanced control techniques, such as adaptive control [11], linear quadratic Gaussian with loop transfer recovery approach [1], H_2 control [6], robust and perfect tracking (RPT) [4], mode switching control [9], composite nonlinear feedback control [2,3], to name a few.

Although these control techniques have significantly improved the performance of HDD servo systems, more challenges still lie ahead as the new generation HDDs impose a more stringent TMR budget for track following. It is known that torque disturbances play an adverse role in HDD track following tasks. The so-called torque disturbances, which include bias torque due to flex cable, pivot bearing friction and hysteresis, as well as other unmodeled dynamics, have conventionally been treated as a lumped disturbance or even ignored when a servo controller is being designed. This may be acceptable in those old drives with low track density. However, for the drives of the new generation, where the TMR budget is at the scale of nanometer, the adverse effects induced by torque disturbances become conspicuous, and performance degradation will occur. To solve this problem, torque disturbances, especially those dominant contributing factors, should be sufficiently modeled and identified at the modeling stage, and integrated into the controller design. For those residual and unmodeled disturbances, an appropriate controller design methodology should be used to minimize their effects on the closed-loop performance. This is the motivation for the current work. In this paper, we present the design of a robust track following controller for a microdrive using the RPT control approach together with a nonlinear pre-compensation. The new design yields a very satisfactory result.

The outline of the paper is organized as follows. A comprehensive model for a microdrive is presented in Section 2, which explicitly captures the characteristics of flex cable nonlinearity and pivot bearing friction. In Section 3, we apply the RPT control methodology combined with a integral and nonlinear torque compensation to design a tracking controller for the microdrive. Simulation and experimental results are given in Section 4. Finally, we draw some concluding remarks in Section 5.

2. Model of a micro hard disk drive

Typically, an HDD servo system uses a voice-coil-motor (VCM) to actuate the R/W recording arm assembly (see Fig. 1). The VCM is a typical DC motor that translates an input current into a force or acceleration. Its frequency domain response without considering friction and nonlinearities matches very well to that of a double integrator at low-medium frequency range, typically from DC to somewhere around 1.5 kHz, and has many high frequency resonant modes. The double integrator model has intensively been used for HDD servo system design for quite some time and it seems to work well for larger drives. Unfortunately, this approximated model is not fine enough for capturing the dynamic characteristics of hard disk drives of the new generation, which demonstrate more noticeable nonlinear and frictional behavior. Some attempts have been made to model and compensate such nonlinearities in the VCM actuator (see, for example, [5,8,12]).

In [8], the so-called physical effect approach was utilized to determine the structures of nonlinearities and friction associated with the VCM actuator in a typical microdrive. Then, a Monte Carlo process was employed to identify parameters in the structured model. These procedures resulted in a comprehensive HDD actuator model which explicitly incorporates the nonlinear effects of the flex cable and the pivot bearing friction. The model (omitting high frequency resonant modes) is given as follows:

$$
\left.
\begin{aligned}
&\ddot{y} = b(u - \widetilde{T}_c) - \widetilde{T}_f, \\
&\widetilde{T}_f = \begin{cases}
T_n, & \dot{y} \neq 0, \\
\widetilde{T}_e, & \dot{y} = 0 \ \text{and} \ |\widetilde{T}_e| \leqslant \widetilde{T}_s, \\
\widetilde{T}_s \operatorname{sgn}(\widetilde{T}_e), & \dot{y} = 0 \ \text{and} \ |\widetilde{T}_e| > \widetilde{T}_s,
\end{cases} \\
&T_n = \left(\left|d_1 b u y + d_2 \dot{y}^2\right| + d_3\right)\operatorname{sgn}(\dot{y}) + d_0 \dot{y}, \\
&\widetilde{T}_e = b[u - \widetilde{T}_c(y)], \\
&\widetilde{T}_s = d_4 b |u_0 y_0| + d_5, \\
&\widetilde{T}_c = a \arctan(cy),
\end{aligned}
\right\}
\tag{1}
$$
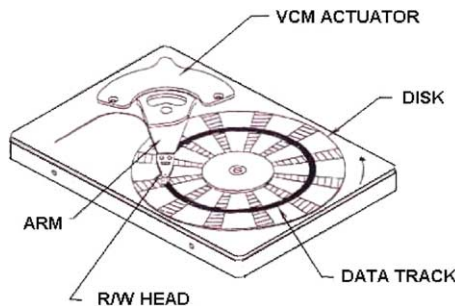
Fig. 1. A typical HDD with a VCM actuator.

where u and y are respectively the control input voltage (in volts) and the displacement (in micrometers) of the R/W head; $\widetilde{T}_f$ is the friction torque and $\widetilde{T}_s$ is the breakaway friction torque with u_0 and y_0 being respectively the corresponding input voltage and the displacement for the case when $\dot{y} = 0$; $\widetilde{T}_c$ is the bias torque induced by the flex cable, which is dependent on the position/displacement of the R/W head and can be measured as the offset torque needed to maintain the R/W head at the corresponding position. Experiments show that $\widetilde{T}_c$ can be matched pretty well by an arctan function of y (see Fig. 2).

An IBM microdrive (model DMDM-10340) was used in the experimental test and its associated parameters have been identified as follows:

$$
\left.
\begin{aligned}
a &= 0.02887, \\
b &= 2.35 \times 10^8, \\
c &= 0.5886, \\
d_0 &= 282.6, \\
d_1 &= 0.005, \\
d_2 &= 0.01, \\
d_3 &= 1.5 \times 10^4, \\
d_4 &= 0.0055, \\
d_5 &= 1.65 \times 10^4.
\end{aligned}
\right\}
\tag{2}
$$
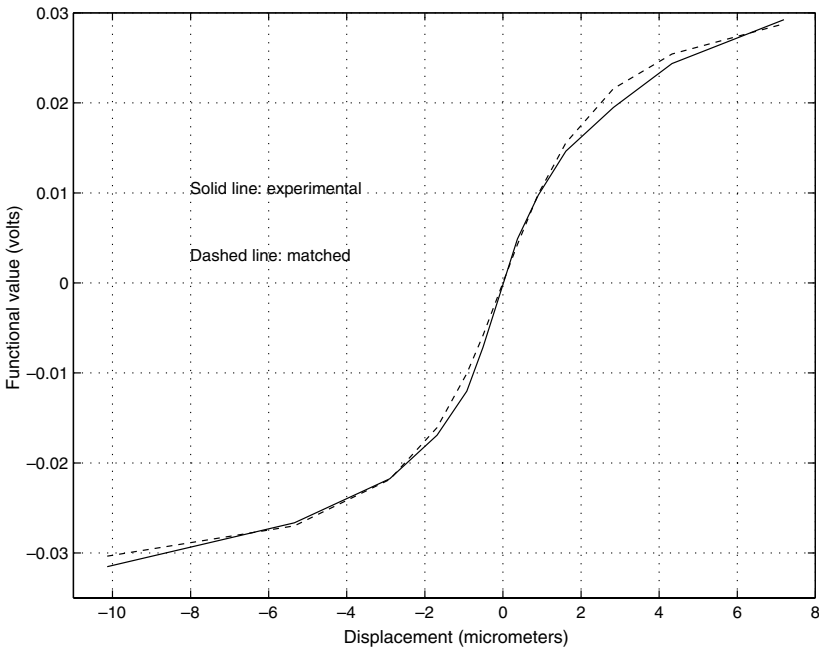
Fig. 2. Nonlinear torque induced by the data flex cable.

The high frequency resonant modes of the VCM actuator have also been identified and approximated as the following transfer function:

$$G_{\text{r.m.}}(s) = G_{\text{r.m.1}}(s)G_{\text{r.m.2}}(s)G_{\text{r.m.3}}(s)G_{\text{r.m.4}}(s)G_{\text{r.m.5}}(s), \tag{3}$$

where

$$G_{\text{r.m.1}}(s) = \frac{0.8709s^2 + 1726s + 1.369 \times 10^9}{s^2 + 1480s + 1.369 \times 10^9}, \tag{4}$$

$$G_{\text{r.m.2}}(s) = \frac{0.9332s^2 - 805.8s + 1.739 \times 10^9}{s^2 + 125.1s + 1.739 \times 10^9}, \tag{5}$$

$$G_{\text{r.m.3}}(s) = \frac{1.072s^2 + 925.1s + 1.997 \times 10^9}{s^2 + 536.2s + 1.997 \times 10^9}, \tag{6}$$

$$G_{\text{r.m.4}}(s) = \frac{0.9594s^2 + 98.22s + 2.514 \times 10^9}{s^2 + 1805s + 2.514 \times 10^9} \tag{7}$$

and

$$G_{\text{r.m.5}}(s) = \frac{7.877 \times 10^9}{s^2 + 6212s + 7.877 \times 10^9}. \tag{8}$$

Verification procedure has also been carried out to confirm that the identified model characterizes very well the behavior of the actual system. Figs. 3 and 4 show that the frequency responses of the actual system and those of the identified model have a close match.
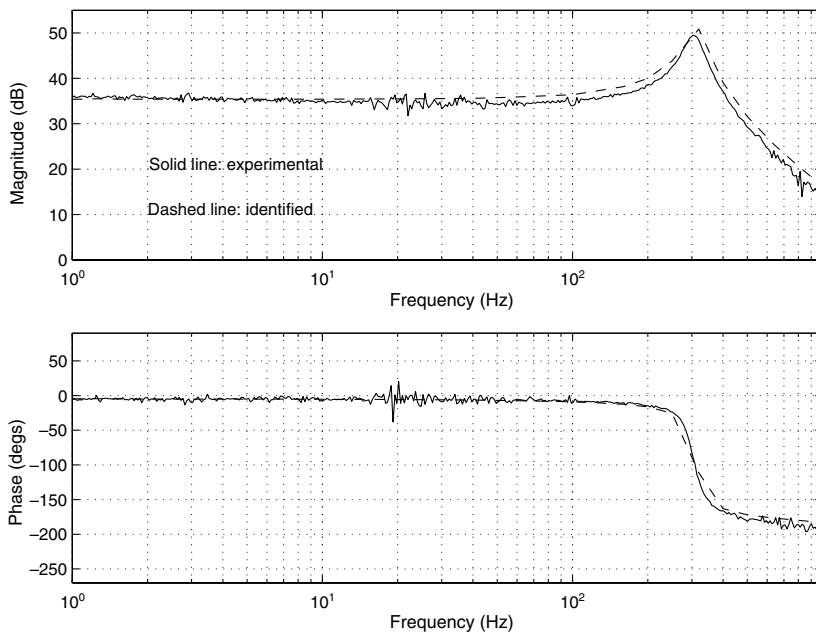
Fig. 3. Frequency responses of the VCM actuator (low frequencies).
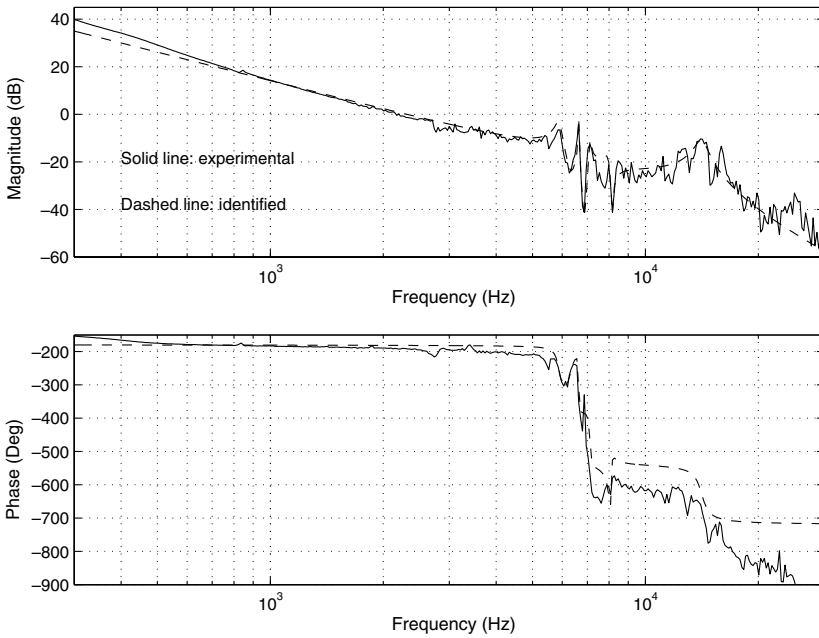
Fig. 4. Frequency responses of the VCM actuator (high frequencies).

3. Design of a microdrive servo controller

The robust and perfect tracking (RPT) technique was introduced in [7] and has been successfully used in designing servo systems for a larger drive (see, for example, [4]). This technique enables control engineers to design a very low-order controller which still results in a closed-loop system with fast tracking speed and low overshoot as well as strong robustness with respect to external disturbances. More specifically, we consider a linear system characterized by a general state-space form:

$$\Sigma : \begin{cases} \dot{x} = Ax + B\bar{u} + Ew, \\ \hat{y} = C_1 x + D_1 w, \\ h = C_2 x + D_2 \bar{u}, \end{cases} \tag{9}$$

where x, $\bar{u}$, w, $\hat{y}$ and h are respectively the state vector, the control input, the external disturbances, the measurement output and the controlled output. A, B, E, C_1, D_1, C_2 and D_2 are constant matrices with appropriate dimensions. Given a target reference vector, r, which has the same number of elements as that of the controlled output, h, the robust and perfect tracking (RPT) control is to design a parameterized controller of the following form:

$$\Sigma_v(\epsilon) : \begin{cases} \dot{x}_v = A_v(\epsilon)x_v + B_y(\epsilon)\hat{y} + B_r(\epsilon)r, \\ \bar{u} = C_v(\epsilon)x_v + D_y(\epsilon)\hat{y} + D_r(\epsilon)r, \end{cases} \tag{10}$$

such that when it is applied to the given system (9),

1. the resulting closed-loop system is internally stable for all $\epsilon \in (0, \epsilon^*]$, where ϵ^* is a positive scalar; and
2. the controlled output h is capable of tracking the target reference r with arbitrary fast settling time in faces of external disturbances and initial conditions, i.e., $\|e\|_p = \|h - r\|_p \to 0$, $p \in [1, \infty)$, as $\epsilon \to 0$.

It was shown in [7] that the above RPT control problem is solvable if and only if the following conditions are satisfied:

1. (A, B) is stabilizable and (A, C_1) is detectable;
2. (A, B, C_2, D_2) is minimum phase and right invertible;
3. $\mathrm{Ker}(C_2) \supseteq C_1^{-1}\{\mathrm{Im}(D_1)\} =: \{v \mid C_1 v \in \mathrm{Im}(D_1)\}$.

Here we note that $\mathrm{Ker}(\cdot)$ and $\mathrm{Im}(\cdot)$ denote respectively the kernel and image of the appropriate matrix. Also, note that for the case when $D_1 = 0$, the last item implies that $\mathrm{Ker}(C_2) \supset \mathrm{Ker}(C_1)$.

In what follows, we proceed to design an HDD tracking controller using the RPT control technique together with some additional enhancements. To do this, we first need to recast the HDD servo problem into the RPT framework. It is noted that the identified HDD model of (1) actually represents a second order system with nonlinear disturbances. Experimental observation shows that flex cable nonlinearity is more influential than pivot bearing friction. As a natural practice and the first step of controller design, we compensate the term of flex cable nonlinearity identified. Next, since the model of friction is somewhat messy, we choose to tick out the viscous friction component (the linear part) and incorporate it into the second order model while treating residual components (including other unmodeled torque disturbances) as an unknown lumped disturbance d_i. To be specific, we introduce

$$\bar{u} = u - a \arctan(cy), \tag{11}$$

then the HDD model can be recast as

$$\ddot{y} = a_1 \dot{y} + a_0 y + b(\bar{u} + d_i), \tag{12}$$

where a_0 and a_1 are parameters introduced to cover general second order systems. We define the following state variables:

$$x_1 = y, \quad x_2 = \dot{y}, \quad x_3 = \int (y - r)\, \mathrm{d}t, \tag{13}$$

where r is the reference input, or the desired position of the R/W head. Next, we define the controlled output as

$$h = x_1 + \lambda x_3, \tag{14}$$

where $\lambda > 0$ is a weighting factor. The HDD system can be formulated into the following RPT form:

$$\Sigma : \begin{cases} \dot{x} = Ax + B\bar{u} + Ew, \\ \hat{y} = C_1 x + D_1 w, \\ h = C_2 x + D_2 \bar{u} \end{cases} \quad (15)$$

with

$$x = \begin{pmatrix} x_1 \\ x_2 \\ x_3 \end{pmatrix}, \quad w = \begin{pmatrix} d_i \\ r \end{pmatrix}, \quad \hat{y} = \begin{pmatrix} x_1 \\ x_3 \end{pmatrix}, \quad (16)$$

$$A = \begin{bmatrix} 0 & 1 & 0 \\ a_0 & a_1 & 0 \\ 1 & 0 & 0 \end{bmatrix}, \quad B = \begin{bmatrix} 0 \\ b \\ 0 \end{bmatrix}, \quad E = \begin{bmatrix} 0 & 0 \\ b & 0 \\ 0 & -1 \end{bmatrix} \quad (17)$$

and

$$C_1 = \begin{bmatrix} 1 & 0 & 0 \\ 0 & 0 & 1 \end{bmatrix}, \quad D_1 = \begin{bmatrix} 0 & 0 \\ 0 & 0 \end{bmatrix}, \quad C_2 = [1 \quad 0 \quad \lambda], \quad D_2 = 0. \quad (18)$$

It can be readily verified that the solvability conditions of the above RPT control are satisfied. The RPT control methodology can be applied to solve the above HDD servo problem.

Note that in HDD servo systems, the dominant task is set point tracking, i.e., to move the R/W head to a desired track, which corresponds to a step reference input characterized by

$$\dot{r}(t) = r \cdot \delta(t). \quad (19)$$

Following the design procedure of [7], we obtain a reduced order measurement feed-back controller

$$\Sigma_v(\epsilon) : \begin{cases} \dot{x}_v = A_v(\epsilon) x_v + B_y(\epsilon) \hat{y} + B_r(\epsilon) r, \\ \bar{u} = C_v(\epsilon) x_v + D_y(\epsilon) \hat{y} + D_r(\epsilon) r \end{cases} \quad (20)$$

with

$$\left. \begin{aligned} A_v(\epsilon) &= -\left(a_1 + \lambda + L + \frac{2\zeta\omega}{\epsilon} \right), \\ B_y(\epsilon) &= -\left[(a_1 + \lambda + L)\left(a_1 + L + \frac{2\zeta\omega}{\epsilon} \right) + \frac{\omega^2}{\epsilon^2} \quad \frac{\omega^2\lambda}{\epsilon^2} \right], \\ B_r(\epsilon) &= \frac{\omega^2}{\epsilon^2} + \frac{2\zeta\omega\lambda}{\epsilon}, \\ C_v(\epsilon) &= -\frac{1}{b}\left(a_1 + \lambda + \frac{2\zeta\omega}{\epsilon} \right), \\ D_y(\epsilon) &= -\frac{1}{b}\left[a_0 + (a_1 + \lambda)(a_1 + L) + \frac{\omega^2}{\epsilon^2} + (a_1 + \lambda + L)\frac{2\zeta\omega}{\epsilon} \quad \frac{\omega^2\lambda}{\epsilon^2} \right], \\ D_r(\epsilon) &= \frac{1}{b}\left(\frac{\omega^2}{\epsilon^2} + \frac{2\zeta\omega\lambda}{\epsilon} \right), \end{aligned} \right\} \quad (21)$$

where ϵ is a tuning parameter that can be tuned to achieve a desired level of performance; ζ and ω are respectively the damping ratio and natural frequency of the supposedly dominant closed-loop conjugate poles; $L > 0$ is corresponding to the reduced order observer pole at $-L$. Noting that x_3 is in fact a part of the actual controller, and combining (11) and (20), we arrive at the following final controller to be implemented onto the real system:

$$\Sigma_{\mathrm{c}}(\epsilon) : \begin{cases} \dot{x}_{\mathrm{c}} = A_{\mathrm{c}}(\epsilon)x_{\mathrm{c}} + B_{\mathrm{c}}(\epsilon)\begin{pmatrix} y \\ r \end{pmatrix}, \\ u = C_{\mathrm{c}}(\epsilon)x_{\mathrm{c}} + D_{\mathrm{c}}(\epsilon)\begin{pmatrix} y \\ r \end{pmatrix} + a\arctan(cy) \end{cases} \tag{22}$$

with

$$\left. \begin{aligned} A_{\mathrm{c}}(\epsilon) &= \begin{bmatrix} -\left(a_1 + \lambda + L + \dfrac{2\zeta\omega}{\epsilon}\right) & -\dfrac{\omega^2\lambda}{\epsilon^2} \\ 0 & 0 \end{bmatrix}, \\ B_{\mathrm{c}}(\epsilon) &= \begin{bmatrix} B_{\mathrm{c}11} & \dfrac{2\zeta\omega\lambda}{\epsilon} + \dfrac{\omega^2}{\epsilon^2} \\ 1 & -1 \end{bmatrix}, \\ C_{\mathrm{c}}(\epsilon) &= -\dfrac{1}{b}\left[a_1 + \lambda + \dfrac{2\zeta\omega}{\epsilon}, \quad \dfrac{\omega^2\lambda}{\epsilon^2} \right], \\ D_{\mathrm{c}}(\epsilon) &= -\dfrac{1}{b}\left[D_{\mathrm{c}11}, \quad -\dfrac{\omega^2}{\epsilon^2} - \dfrac{2\zeta\omega\lambda}{\epsilon} \right], \end{aligned} \right\} \tag{23}$$

where

$$B_{\mathrm{c}11} = -(a_1 + \lambda + L)\left(a_1 + L + \dfrac{2\zeta\omega}{\epsilon}\right) - \dfrac{\omega^2}{\epsilon^2} \tag{24}$$

and

$$D_{\mathrm{c}11} = a_0 + (a_1 + \lambda)(a_1 + L) + \dfrac{\omega^2}{\epsilon^2} + (a_1 + \lambda + L)\dfrac{2\zeta\omega}{\epsilon}. \tag{25}$$

The following remarks are in order.

Remark 3.1. Note that $\Sigma_{\mathrm{c}}(\epsilon)$ is a closed-form controller parameterized by ϵ, ζ, ω, λ and L. In the actual implementation, we have to take into consideration the physical limitation of the HDD servo system, such as actuator saturation and resonant modes. The parameterized design enables us to easily tune the controller parameters to achieve a good performance.

Remark 3.2. In the formulation of the HDD servo controller design, we have defined the controlled output to be $h = x_1 + \lambda x_3 = x_1 + \lambda\int e$. This is important for the solvability of the RPT problem with integral augmentation. It can be verified that the transfer function from reference r (the desired track) to output displacement y of R/W head is given by

$$H_{yr}(s) = \frac{\omega(\omega + 2\zeta\omega\lambda)}{\epsilon^2} \cdot \frac{(s+L)\left(s + \dfrac{\omega\lambda}{\omega + 2\zeta\epsilon\lambda}\right)}{(s+L)\left(s^2 + \dfrac{2\zeta\omega s}{\epsilon} + \dfrac{\omega^2}{\epsilon^2}\right)(s+\lambda)}. \tag{26}$$

As expected, there is a pole/zero cancellation at $-L$. There are three poles, respectively, at $-\lambda$, $-\frac{\zeta\omega}{\epsilon} \pm j\frac{\omega}{\epsilon}\sqrt{1-\zeta^2}$, and one zero at $-\frac{\omega\lambda}{\omega+2\zeta\epsilon\lambda}$. As $\epsilon \to 0$, $\frac{\omega\lambda}{\omega+2\zeta\epsilon\lambda} \to \lambda$, there will be an asymptotic pole/zero cancellation at $-\lambda$, and the closed-loop system will behave like a second order system. Finally, it is easy to verify $H_{yr}(0) = 1$, which guarantees a zero steady-state error for set point tracking.

Remark 3.3. The nonlinear compensation term in our controller directly cancels the major part of the torque disturbances in the microdrive. We note that without a clear model of these disturbances, it might be necessary to employ a controller with higher bandwidth to reject the disturbances. However, as the bandwidth is pushed higher, more noises will enter into the control loop, which may result in performance degradation and even trigger the plant resonant modes. By using a nonlinear compensation, we are able to properly design a moderately high bandwidth controller, which maintains a good balance between time domain and frequency domain specifications.
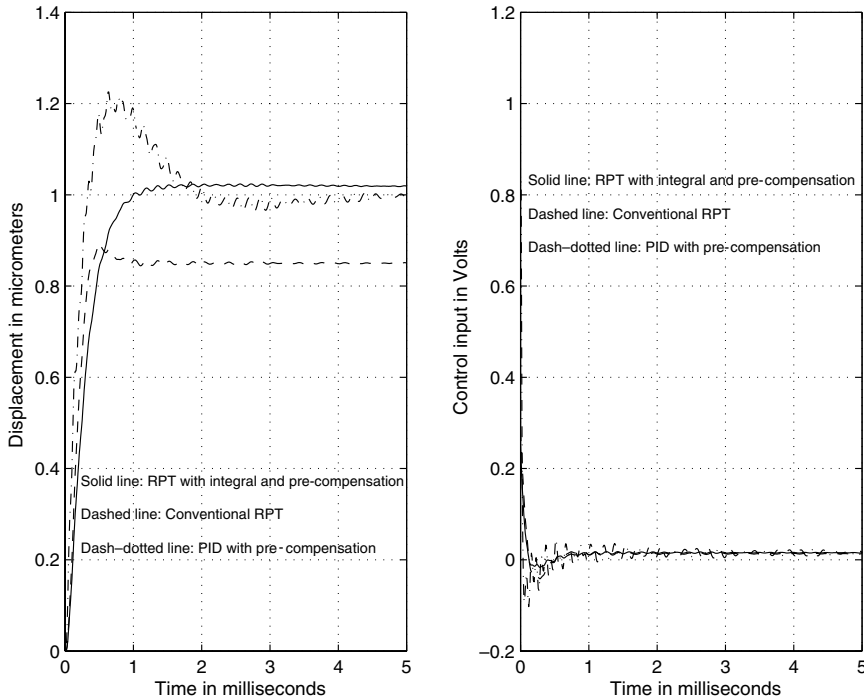
Fig. 5. Simulation result.

Remark 3.4. In our design of the HDD tracking controller, we only utilize the nominal model of the microdrive. However, it is crucial to include the high frequency resonant modes in simulation before one carries out the implementation of the controller to the actual hardware. The simulation result obtained in the next section is done with all the resonant modes of (3)–(8) being included.

4. Simulation and experimental results

Simulations and experiments are carried out to evaluate the performance of the designed controller. For experiment, we use an open microdrive (IBM model DMDM-10340), whose characteristics are as given in Section 2. The only measurable output is the relative displacement of the R/W head, which is measured by a Laser Doppler Vibrometer (LDV). Control algorithm is implemented on a dSpace DSP board installed in a personal computer. The sampling rate is chosen to be 20 kHz, a typical frequency used in HDD servo systems. For this specific microdrive with track density of 35 kTPI, its track pitch is around 0.7 μm. Hence, the TMR budget, which is defined here as 3% of track pitch, is about 0.02 μm. A desirable controller is expected to bring the R/W head into the 0.02 μm neighborhood of the target track as soon as possible.
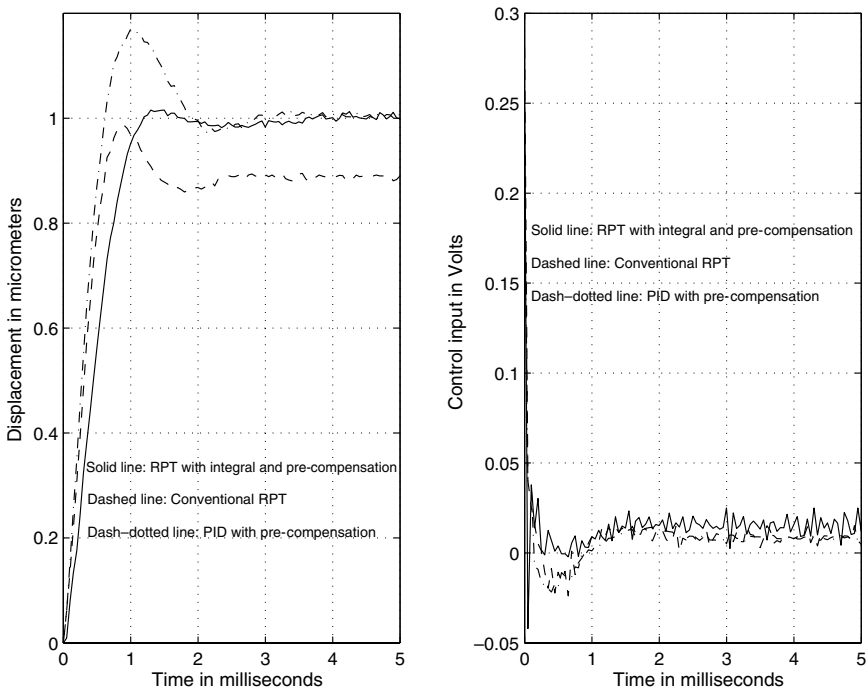
Fig. 6. Experimental result.

Since $\Sigma_c(\epsilon)$ is a parameterized controller, we can easily tune its parameters, ϵ, ζ, ω, λ and L, to achieve satisfactory results. For this microdrive, we have

$$b = 2.35 \times 10^8, \quad a_0 = 0, \quad a_1 = -282.6, \quad a = 0.02887, \quad c = 0.5886. \tag{27}$$

By online tuning, we find that the following controller parameters give the best performance:

$$\epsilon = 1, \quad \zeta = 1.2, \quad \omega = 2400\pi, \quad \lambda = 80, \quad L = 6000. \tag{28}$$

The final controller is then given by

$$\begin{cases} \dot{x}_c = \begin{bmatrix} -2.3893 \times 10^4 & -4.5479 \times 10^9 \\ 0 & 0 \end{bmatrix} x_c + \begin{bmatrix} -1.949 \times 10^8 & 5.8297 \times 10^7 \\ 1 & -1 \end{bmatrix} \begin{pmatrix} y \\ r \end{pmatrix}, \\ \bar{u} = \begin{bmatrix} -7.614 \times 10^{-5} & -19.353 \end{bmatrix} x_c + \begin{bmatrix} -0.6834 & 0.2481 \end{bmatrix} \begin{pmatrix} y \\ r \end{pmatrix} \end{cases} \tag{29}$$

and

$$u = \bar{u} + 0.02887 \arctan(0.5886y). \tag{30}$$
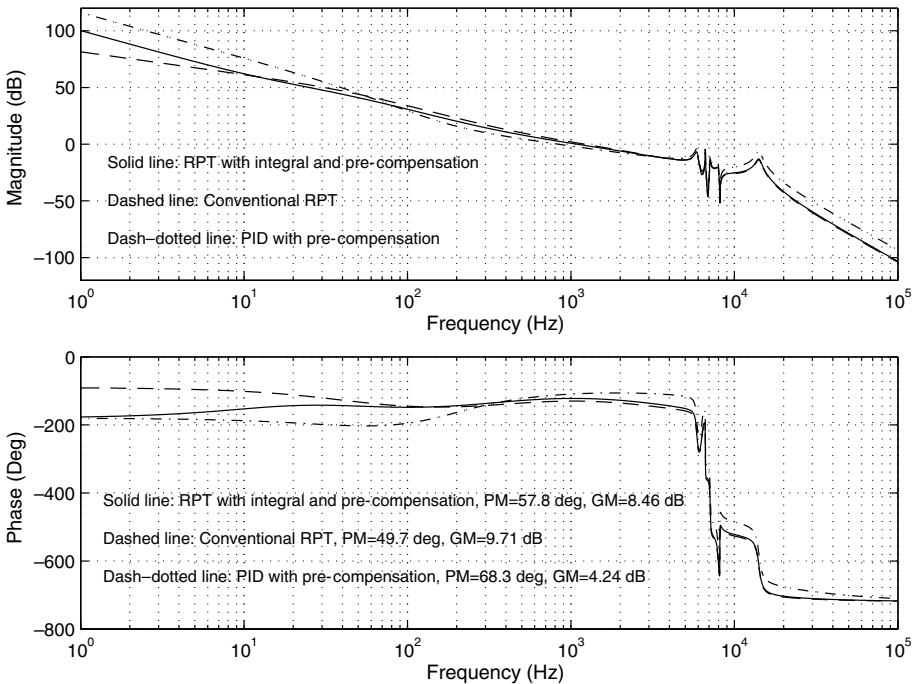
Fig. 7. Bode plot of the open-loop transfer functions.

For comparison, we design a conventional RPT controller, which does not include integral enhancement and nonlinear compensation. The conventional RPT controller is given by

$$\dot{x}_v = -\left(L + \frac{2\zeta\omega}{\epsilon}\right)x_v - \left(L^2 + \frac{2\zeta\omega L}{\epsilon} + \frac{\omega^2}{\epsilon^2}\right)y + \frac{\omega^2}{\epsilon^2}r \tag{31}$$

and

$$u = -\frac{1}{b}\left[\frac{2\zeta\omega}{\epsilon}x_v + \left(\frac{2\zeta\omega L}{\epsilon} + \frac{\omega^2}{\epsilon^2}\right)y - \frac{\omega^2}{\epsilon^2}r\right] \tag{32}$$

with the following best tuned parameters: $\epsilon = 1$, $\zeta = 0.8$, $\omega = 2600\pi$, $L = 6000$.

To compare our result with classical approaches, we also design a PID controller with the nonlinear pre-compensation,

$$\begin{pmatrix} \dot{z} \\ \dot{x}_d \end{pmatrix} = \begin{bmatrix} 0 & 0 \\ 0 & -10^5 \end{bmatrix}\begin{pmatrix} z \\ x_d \end{pmatrix} + \begin{bmatrix} 1 \\ 1 \end{bmatrix}(r - y) \tag{33}$$

and

$$u = 2.181(r - y) + 30z - 2.139 \times 10^5 x_d + 0.02887\arctan(0.5886y). \tag{34}$$

For simulation verifications, we use the nonlinear model of the HDD in (1)–(8) instead. Simulation and actual implementation results of Figs. 5 and 6 show that
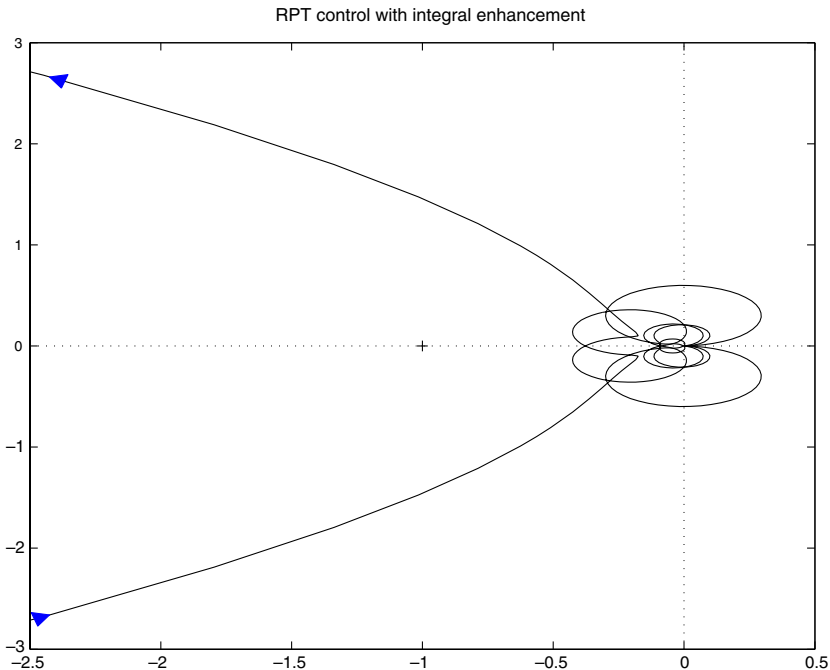
Fig. 8. Nyquist plot of the open-loop transfer function (RPT with integration).
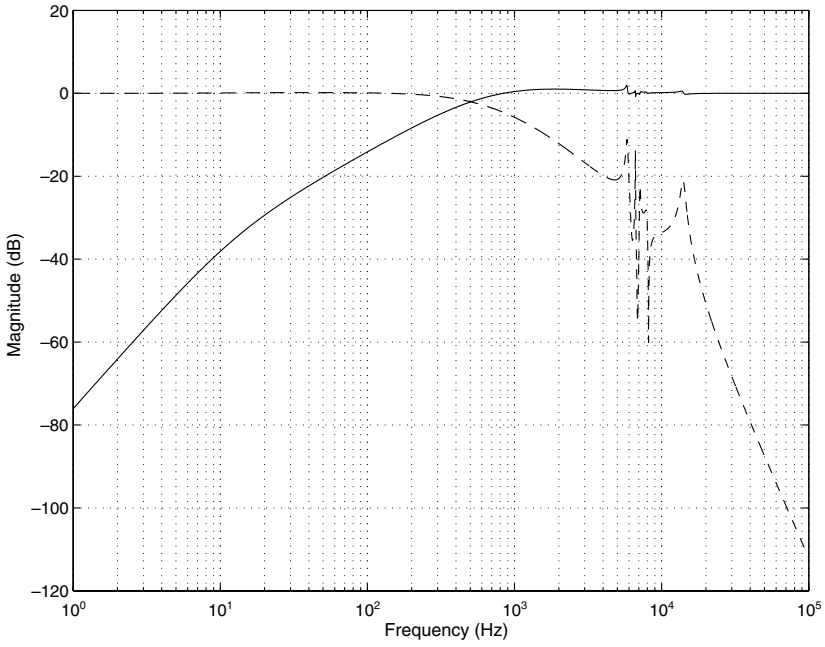
Fig. 9. Plot of the sensitivity and complementary sensitivity functions (RPT with integration).
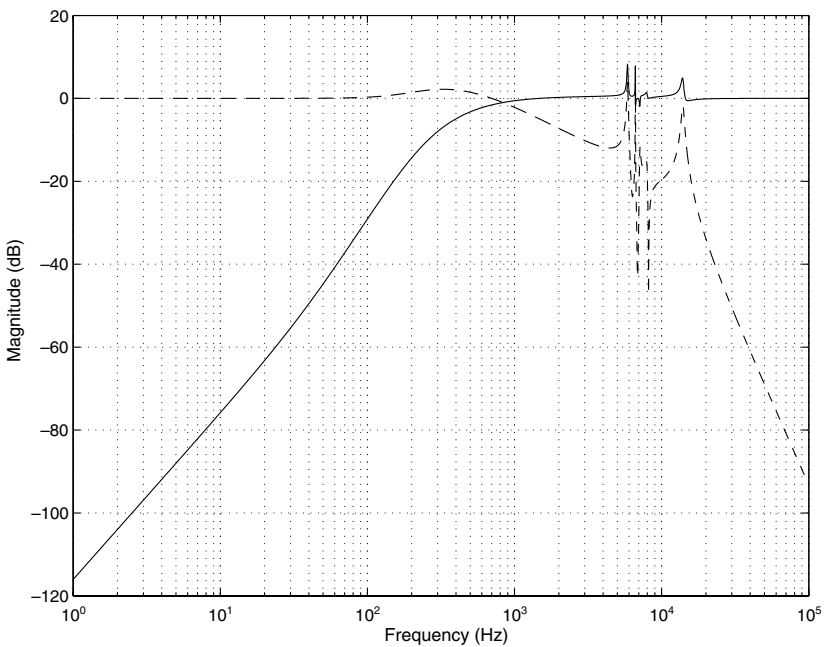
Fig. 10. Plot of the sensitivity and complementary sensitivity functions (PID control).

the RPT control with the nonlinear compensation and the additional integral action yields a much better performance compared to those of the conventional RPT controller and the classical PID controller. The frequency domain characteristics are shown in Figs. 7–10. The new design has an impressive gain and phase margins as well compared to the classical approach.

5. Concluding remarks

In this paper, we have presented the design of a microdrive servo controller using the robust and perfect tracking control methodology together with an integral and nonlinear compensation. The design was carried out based on a comprehensive VCM actuator model, in which the characteristics of pivot bearing friction and flex cable nonlinearity are explicitly identified. Simulation and experiment results show that our design is capable of achieving faster settling and eliminating static bias.

Acknowledgments

References

[1] Chang JK, Ho HT. LQG/LTR frequency loop shaping to improve TMR budget. IEEE Trans Magn 1999;35:2280–2.
[2] Chen BM, Lee TH, Venkataramanan V. Hard disk drive servo systems. New York, London: Springer-Verlag; 2002.
[3] Chen BM, Lee TH, Peng K, Venkataramanan V. Composite nonlinear feedback control for linear systems with input saturation: theory and an application. IEEE Trans Automat Control 2003;48:427–39.
[4] Goh TB, Li Z, Chen BM, Lee TH, Huang T. Design and implementation of a hard disk drive servo system using robust and perfect tracking approach. IEEE Trans Control Syst Technol 2001;9:221–33.
[5] Gong JQ, Guo L, Lee HS, Yao B. Modeling and cancellation of pivot nonlinearity in hard disk drives. IEEE Trans Magn 2002;38:3560–5.
[6] Li Z, Guo G, Chen BM, Lee TH. Optimal control design to achieve highest track-per-inch in hard disk drives. J Inform Storage Process Syst 2001;3:27–41.
[7] Liu K, Chen BM, Lin Z. On the problem of robust and perfect tracking for linear systems with external disturbances. Int J Control 2001;74:158–74.
[8] Peng K, Cheng G, Chen BM, Lee TH. Comprehensive modeling of friction in a hard disk drive actuator. In: Proceedings of the 2003 american control conference, Denver, USA, 2003. p. 1380–5.
[9] Venkataramanan V, Chen BM, Lee TH, Guo G. A new approach to the design of mode switching control in hard disk drive servo systems. Control Eng Practice 2002;10:925–39.
[10] White M, Tomizuka M, Smith C. Improved track following in magnetic disk drives using a disturbance observer. IEEE/ASME Trans Mech 2000;5:3–11.

[11] Wu D, Guo G, Chong TC. Adaptive compensation of microactuator resonance in hard disk drives. IEEE Trans Magn 2000;36:2247–50.
[12] Yan T, Lin R. Experimental modeling and compensation of pivot nonlinearity in hard disk drives. IEEE Trans Magn 2003;39:1064–9.